JOURNAL OF BACTERIOLOGY, July 2006, p. 4841–4850 Vol. 188, No. 13
0021-9193/06/$08.00+0 doi:10.1128/JB.00326-06
Copyright © 2006, American Society for Microbiology. All Rights Reserved.

Polar Localization of the Autotransporter Family of Large Bacterial Virulence Proteins

Sumita Jain,[1] Peter van Ulsen,[2] Inga Benz,[3] M. Alexander Schmidt,[3] Rachel Fernandez,[4] Jan Tommassen,[2] and Marcia B. Goldberg[1]*

Division of Infectious Diseases, Department of Medicine, Massachusetts General Hospital/Harvard Medical School, Cambridge, Massachusetts[1]; Department of Molecular Microbiology, Institute of Biomembranes, Utrecht University, Utrecht, The Netherlands[2]; Institut für Infektiologie, Zentrum für Molekularbiologie der Entzündung, Münster, Germany[3]; and Department of Microbiology and Immunology, Life Sciences Centre, University of British Columbia, Vancouver, British Columbia V6T 1Z3, Canada[4]

Received 6 March 2006/Accepted 17 March 2006

Autotransporters are an extensive family of large secreted virulence-associated proteins of gram-negative bacteria. Secretion of such large proteins poses unique challenges to bacteria. We demonstrate that autotransporters from a wide variety of rod-shaped pathogens, including IcsA and SepA of *Shigella flexneri*, AIDA-I of diffusely adherent *Escherichia coli*, and BrkA of *Bordetella pertussis*, are localized to the bacterial pole. The restriction of autotransporters to the pole is dependent on the presence of a complete lipopolysaccharide (LPS), consistent with known effects of LPS composition on membrane fluidity. Newly synthesized and secreted BrkA is polar even in the presence of truncated LPS, and all autotransporters examined are polar in the cytoplasm prior to secretion. Together, these findings are consistent with autotransporter secretion occurring at the poles of rod-shaped gram-negative organisms. Moreover, NalP, an autotransporter of spherically shaped *Neisseria meningitidis* contains the molecular information to localize to the pole of *Escherichia coli*. In *N. meningitidis*, NalP is secreted at distinct sites around the cell. These data are consistent with a model in which the secretion of large autotransporters occurs via specific conserved pathways located at the poles of rod-shaped bacteria, with profound implications for the underlying physiology of the bacterial cell and the nature of bacterial pathogen-host interactions.

Secretion of large proteins through the layers of the gram-negative bacterial envelope poses a challenge to the cell. To reach the cell surface, the protein must traverse two lipid bilayers, an intervening periplasmic space, and a peptidoglycan mesh. The largest family of secreted proteins in gram-negative bacteria is the autotransporter family, with more than 700 members thought to exist (35). Autotransporters are present throughout the gram-negative bacterial world, including among members of the α-, β-, γ-, and ε-proteobacteria. They are expressed in many pathogens in which they are involved in the pathogenesis of disease (21) but are also found in nonpathogens (48). Autotransporters have a wide variety of functions, including adhesion, polymerization of host cell actin, vacuolating or nonvacuolating cytotoxicity, serum resistance, and protease, lipase, or esterase activity. Secretion of these proteins allows their direct contact with the cellular molecules of the eukaryotic host that are targets of their activities (22).

Autotransporters are large proteins, generally 90 to 200 kDa. They share a common domain organization that includes an amino-terminal signal peptide, a divergent functional domain that is exposed at the bacterial surface, and a conserved carboxy-terminal translocation domain that forms a β-barrel in the outer membrane (34) (Fig. 1A). Secretion across the inner membrane involves the Sec apparatus (7, 43, 47). The large size of autotransporters poses challenges for their translocation across the peptidoglycan mesh, the pores of which may have a radius of only 3.1 nm (50), which would permit the passage of globular proteins up to 100 kDa in size. The translocation domain is required for the passage of the functional domain across the outer membrane. For the immunoglobulin A protease of *Neisseria meningitidis*, this translocation step has been shown to also involve the outer membrane protein Omp85 (51); whether Omp85 or Omp85 homologs are required in the translocation of autotransporters generally is as yet unknown. Little else is known about the mechanisms involved in secretion of these large proteins across the peptidoglycan sacculus and the outer membrane. In the present study, we demonstrate that autotransporters from a wide variety of gram-negative bacteria are localized to the bacterial pole, suggesting that a specific polar secretion pathway that mediates their secretion across the periplasm and the outer membrane may exist.

* Corresponding author. Mailing address: Massachusetts General Hospital, 65 Landsdowne St., Cambridge, MA 02139. Phone: (617) 768-8740. Fax: (617) 768-8738. E-mail: mgoldberg1@partners.org.

MATERIALS AND METHODS

Bacterial strains, plasmids, and growth conditions. Bacterial strains and plasmids used in the present study are listed in Table 1. *Escherichia coli* and *Shigella flexneri* strains were routinely maintained in LB medium at 37°C. *Bordetella* strains were grown on BG agar plates supplemented with 15% defibrinated sheep's blood or in Stainer-Scholte's broth (45) plus supplements. *N. meningitidis* strains were grown at 37°C, under limited oxygen conditions (5% CO_2), on GC agar plates supplemented with Vitox or in liquid tryptic soy broth. For induction of the expression of LbpA in wild-type *N. meningitidis*, the iron chelator EDDHA [ethylene-diamine(*o*-hydroxyphenylacetic)acid] was added to the growth media. Antibiotics, where appropriate, were added to the following concentrations: ampicillin, 100 μg/ml; and chloramphenicol, 10 μg/ml (for *N. meningitidis*) or 25 μg/ml (for *E. coli*).

Downloaded from https://journals.asm.org/journal/jb on 07 August 2023 by 68.181.16.190.

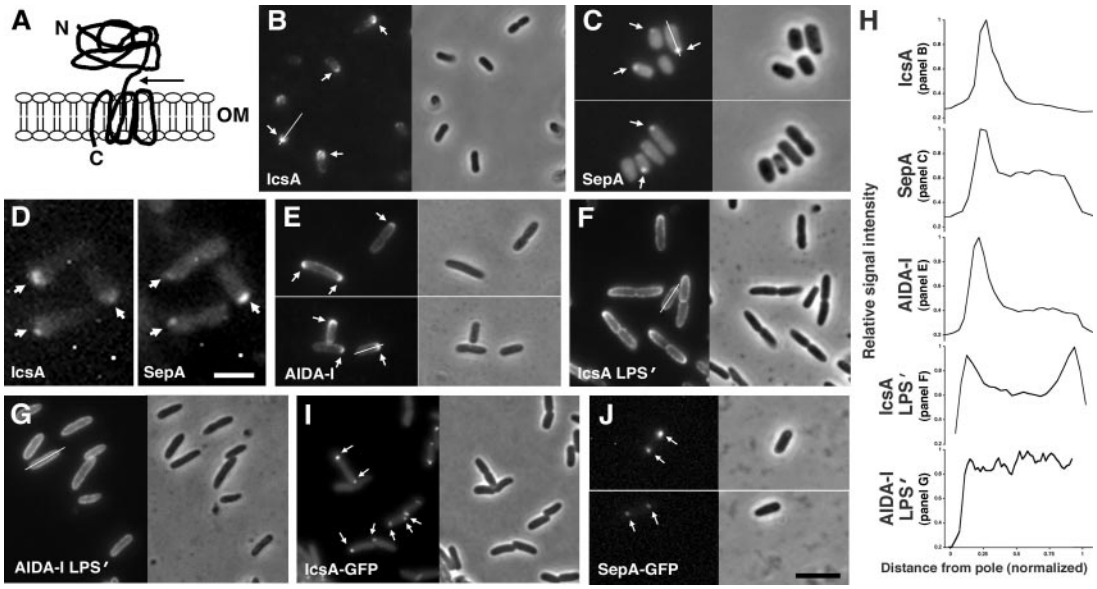

FIG. 1. Localization of autotransporter proteins of *Enterobacteriaceae* to the bacterial pole. (A) Orientation of autotransporter protein in the bacterial outer membrane (OM). The mature amino-terminal functional domain is exposed at the bacterial surface after its translocation is mediated by the carboxy-terminal OM β-barrel domain. N, amino terminus; C, carboxy terminus. (B and C) The *S. flexneri* autotransporters IcsA (B) and SepA (C) on the surface of intact wild-type *S. flexneri* (strain 2457T). (D) IcsA and SepA at the same pole of individual wild-type *S. flexneri* (strain 2457T), localized by using monoclonal antibodies to IcsA and polyclonal antibodies to SepA. (E and G) Pathogenic *E. coli* (DAEC) autotransporter AIDA-I on the surface of intact wild-type *E. coli* 2443 cells (strain 2443 *ompT* pIB264), which express a complete LPS (E), or on the surface of intact *E. coli* K-12 (strain MBG263/pIB264) (G). (F) IcsA on the surface of *E. coli* K-12 (strain MBG263/pMBG270). (H) Plots of signal intensity (*y* axis) as a function of distance from cell pole along the long axis (*x* axis) for representative single cells (indicated by white line) from each of panels B and C and E to G. (I and J) GFP fusion to the cytoplasmic derivative of IcsA (strain BS103/pBAD24-*icsA*$_{1\text{-}24/53\text{-}757}$::*gfp*) (I) or SepA (strain BS103/pBAD24-*sepA*$_{1\text{-}24/57\text{–}1042}$::*gfp*) (J). Except for GFP (I and J), the detection of signals from each protein was done by indirect immunofluorescence. Arrows, polarly localized autotransporter protein. B and C, E to G, and I and J: left panel, fluorescence image; right panel, phase-contrast image. Size bars: B and C, E to G, and I and J (bar shown in panel J), 5 μm; D, 3 μm.

Construction of plasmids. pSU20-*sepA* is the entire coding sequence of SepA and the *sepA* promoter carried on plasmid pSU20 (1). The *sepA* gene and promoter was amplified by PCR using the oligonucleotide primers MBG1106 and MBG1107 (Table 2) and, as a template, genomic DNA from *S. flexneri* strain 2457T. The PCR product was digested with PvuII and cloned into the EcoRV site of pBR322, in an orientation opposite to that of the tetracycline resistance cassette, to generate the plasmid pBR322-*sepA*. The NheI-ClaI fragment that contains the *sepA* gene was then subcloned into the XbaI and ClaI sites of pSU20 to obtain pSU20-*sepA*.

IcsA and SepA, like most autotransporters, contain unusually long secretion signals, with approximately 25 residues at the extreme N terminus lying N terminal to the Sec recognition motif. pBAD24-*icsA*$_{1\text{-}24/53\text{-}757}$::*gfp* contains the coding sequence for the *S. flexneri* IcsA signal peptide, from which the coding sequence for the typical Sec recognition motif (amino acids 25 to 52) has been deleted, upstream and in-frame with the coding sequence for the IcsA functional domain, upstream and in-frame with *gfp*. The expression of the gene fusion is under the control of an arabinose-inducible promoter. The plasmid was generated by three-step PCR, as follows. The 87 bp that encode IcsA amino acids 1 to 24 were amplified by PCR using the oligonucleotide primers SJ26 and SJ27 (Table 2), and the 156 bp that encode IcsA amino acids 53 to 104 were amplified using the oligonucleotide primers SJ28 and SJ4 (Table 2), with, as a template, pBAD24-*icsA*$_{1\text{-}757}$::*gfp* (9). Since oligonucleotide SJ27 is complementary to oligonucleotide SJ28, the PCR products from these two reactions contained a complementary sequence. In a third round of PCR, this complementary sequence was used to generate a product that creates an in-frame fusion between the DNA fragment encoding IcsA amino acids 1 to 24 and the DNA fragment encoding IcsA amino acids 53 to 104. This final PCR product was digested with EcoRI and XbaI (sites included in oligonucleotide primers SJ26 and SJ4, respectively) and shuttled into the EcoRI and XbaI sites of pBAD24-*icsA*$_{1\text{-}757}$::*gfp* (9), thereby replacing *icsA*$_{1\text{-}757}$ with *icsA*$_{1\text{-}24/57\text{-}757}$ and generating pBAD24-*icsA*$_{1\text{-}24/53\text{-}757}$::*gfp*. The expression of each gene fusion in pBAD24 is under the control of an arabinose-inducible promoter.

pBAD24-*sepA*$_{1\text{-}1042}$::*gfp* contains the coding sequence for the signal peptide and functional domain of *S. flexneri* SepA upstream and in-frame with *gfp*. Expression of the gene fusion is under the control of an arabinose-inducible promoter. The plasmid was generated by PCR amplification of the 5′ 870 bp of the *sepA* coding sequence as a BspHI-Bsu36I fragment, using oligonucleotides SJ11 and SJ12 (Table 2) and *S. flexneri* strain 2457T genomic DNA as a template, and cloning of this fragment into the NcoI-Bsu36I sites of pBAD24-*sepA*$_{57\text{-}1042}$::*gfp* (9).

pBAD24-*sepA*$_{1\text{-}24/57\text{-}1042}$::*gfp* is a derivative of pBAD24-*sepA*$_{1\text{-}1042}$::*gfp* from which the coding sequence for the typical Sec recognition motif (SepA amino acids 25 to 56) has been deleted. It was generated by using a strategy similar to that used in the construction of pBAD24-*icsA*$_{1\text{-}24/53\text{-}757}$::*gfp*. DNA fragments encoding SepA amino acids 1 to 24 and SepA amino acids 57 to 294 were amplified by PCR, using the oligonucleotide primers SJ11 and SJ23 for amino acids 1 to 24, and SJ24 and SJ12 for amino acids 57 to 294 (Table 2), with, as a template, pBAD24-*sepA*$_{1\text{-}1042}$::*gfp*. Since oligonucleotide SJ23 is complementary to oligonucleotide SJ24, the PCR products from these two reactions contained a complementary sequence. In a third round of PCR, this overlap was used to generate a product that creates an in-frame fusion between the DNA fragment encoding SepA amino acids 1 to 24 and that encoding SepA amino acids 57 to 274. This final PCR product was digested with BspHI and Bsu36I (sites included in oligonucleotide primers SJ11 and SJ12, respectively) and shuttled into the NcoI and Bsu36I sites of pBAD24-*sepA*$_{57\text{-}1042}$::*gfp* (9), thereby replacing *sepA*$_{57\text{-}274}$ with *sepA*$_{1\text{-}24/57\text{-}274}$ and generating pBAD24-*sepA*$_{1\text{-}24/57\text{-}1042}$::*gfp*.

Antibodies used in this study. Antiserum to IcsA, monoclonal antibodies to IcsA, and antiserum to BrkA have been described previously (18, 33, 39). Antiserum to SepA was generated by the immunization of rabbits with the SepA functional domain. The functional domain, which is cleaved and released from the bacterial surface of SepA-expressing cells, was purified from culture supernatants of *E. coli* cells carrying pSU20-*sepA*, which encodes full-length SepA and the *sepA* promoter. Culture supernatants were filtered and concentrated 75-fold to ~500 μg of protein/ml by passage through Amicon centrifuge tubes with a molecular mass cutoff of 100 kDa. The 110-kDa secreted functional domain of SepA, which was the major polypeptide retained by the filter, as detected by Coomassie-stained sodium dodecyl sulfate-polyacrylamide gel electrophoresis (SDS-PAGE), was used for the immunization of rabbits (Covance, Inc.). Im-

Downloaded from https://journals.asm.org/journal/jb on 07 August 2023 by 68.181.16.190.

TABLE 1. Bacterial strains and plasmids used in this study

Bacterial strain or plasmid	Pertinent genotype[a]	Source or reference
Strains		
E. coli 2443 *ompT*	rfb_{O8} *ompT*::Km	32
E. coli BL21(DE3)	DE3 (a λ prophage carrying the T7 RNA polymerase gene under control of p*lac*UV5), *ompT*, expresses O antigen M	Invitrogen
E. coli DH10B	K-12 cloning strain	Gibco BRL
E. coli MBG263	MC1061 *ompT*::Km	19
E. coli MC1061	K-12 strain	30
E. coli JM109(DE3)	K-12 strain with DE3, a λ prophage carrying the T7 RNA polymerase gene under control of p*lac*UV5	NEB
S. flexneri 2457T	Wild-type serotype 2a	27
S. flexneri BS103	2457T cured of the virulence plasmid	29
B. pertussis BBC8	Str^r derivative of wild-type strain W28	14
N. meningitidis CE1449	H44/76 *lbpA*::Erm; Erm^r	36
N. meningitidis H44/76	H44/76	E. Holten
N. meningitidis H44/76 *nalP*	H44/76 *nalP*::Km; Km^r	49
Plasmids		
pBAD24-$icsA_{1\text{-}24/53\text{-}757}$::*gfp*	pBAD24 $icsA_{1\text{-}24/53\text{-}757}$::*gfp*; Amp^r	This study
pBAD24-$sepA_{1\text{-}1042}$::*gfp*	pBAD24 $sepA_{1\text{-}1042}$::*gfp*; Amp^r	This study
pBAD24-$sepA_{1\text{-}24/57\text{-}1042}$::*gfp*	pBAD24 $sepA_{1\text{-}24/57\text{-}1042}$::*gfp*; Amp^r	This study
pBAD24-$sepA_{57\text{-}1042}$::*gfp*	pBAD24 $sepA_{57\text{-}1042}$::*gfp*; Amp^r	9
pDO6935	pBluescript II SK(−) *brkA*; Amp^r	33
pEN300	pFP10 *lacI*^{q} P_{lac}-*nalP*; Cm^r	49
pEN305	pFP10 *lacI*^{q} P_{lac}-*nalP*S^{427}A; Cm^r	49
pFP10-$lbpA_{BNCV}$	pFP10 *lacI*^{q} P_{lac}-$lbpA_{BNCV}$ (*lbpA* from strain BNCV); Cm^r	J. Kortekaas
pIB264	pBR322 *aah aidA*; Amp^r	3
pMBG270	pBR322 *icsA*; Amp^r	28
pPU300	pET11a P_{T7}-*nalP*; Amp^r	49
pPU305	pET11a P_{T7}-*nalP*S^{427}A; Amp^r	49
pSU20-*sepA*	pSU20 *sepA*; Cm^r	This study

[a] Cm^r, chloramphenicol resistance; Amp^r, ampicillin resistance; Erm^r, erythromycin resistance; Str^r, streptomycin resistance; Km^r, kanamycin resistance.

mune serum was affinity purified using SepA polypeptide from filtered culture supernatants. The specificity of the antibody was verified by Western blotting against *Shigella* supernatant proteins from wild-type *S. flexneri*, which expresses SepA, and virulence plasmid-cured *S. flexneri*, which does not express SepA.

Protein expression and detection. The detection of protein on the surface of intact bacteria was performed by indirect immunofluorescence, essentially as described previously (18), or by a modified protocol in which labeling with primary and secondary antibodies is performed prior to fixation. The detection of newly synthesized protein on the surface of intact bacteria was performed by imaging or fixing cells at specific times after induction of expression of the protein in question from an inducible promoter. Although data from some investigators suggests that O antigen along the lengths of *S. flexneri* has greater numbers of repeats (31), this does not block the detection of IcsA with our antiserum, since disruption of the gene encoding the IcsA surface protease leads to detection of IcsA along the lengths of the cell in the absence of alteration of O antigen length or distribution (46).

Antisera to IcsA and SepA were used at a dilution of 1:100, and antiserum to BrkA was used at a dilution of 1:400. For simultaneous labeling of SepA and IcsA, anti-IcsA mouse monoclonal antibody was used at a dilution of 1:100 with a fluorescein isothiocyanate-conjugated anti-mouse secondary antibody, and anti-SepA antiserum was used as described above with a Texas red-conjugated anti-rabbit secondary antibody. Antiserum to AIDA-I (5) was absorbed to *E. coli* 2443 *ompT* prior to use and, for the detection of NalP on *E. coli*, antiserum to the functional domain of NalP (49) was absorbed to *E. coli* BL21(DE3) and/or *E. coli* JM109(DE3) prior to use; for each, the absorbed antiserum was used at a dilution of 1:200. For the detection of NalP on the surface of *N. meningitidis*, antiserum to NalP was used at a dilution of 1:150, and for the detection of LbpA, antiserum r2 to LbpA was used at a dilution of 1:300. For Western blot analysis, in addition to the antisera described above, an antiserum to the β-barrel domain of NalP (34) was used where appropriate. Antiserum to LbpA was a gift from J. Kortekaas.

TABLE 2. Oligonucleotides used in this study

Oligonucleotide	Sequence (5′ to 3′)[a]
MBG1106	AGCATCCCCC**CAGCTG**AACTGGC
MBG1107	CTGGACGGTCA**CAGCTG**AGAAAAGG
SJ4	GT**TCTAGA**TGCATGAGAGGGGTTGGAAGA
SJ11	GG**TCATGA**ACAAAATATATTATCTTAAG
SJ12	GTTAGTT**CCTGAGG**AAAGCA
SJ23	TGCACTGACCGTTGCGCGGGCCAGTTCGGA
SJ24	TCCGAACTGGCCCGCGCAACGGTCAGTGCA
SJ26	AG**GAATTC**ACCATGAATCAAATTCACAAA
SJ27	ACCCGAAAGAGGAGTCGTAGGTAATTCTCC
SJ28	GGAGAATTACCTACGACTCCTCTTTCGGGT

[a] Restriction sites are shown in boldface.

For the detection of newly synthesized BrkA on the surface of intact *Bordetella* cells, the Bvg two-component signal transduction system was first repressed by growth at 30°C in the presence of 50 mM $MgSO_4$ and then activated for specified times by growth at 37°C without $MgSO_4$. For the detection of newly synthesized NalP on the surface of intact *E. coli* cells, NalP was expressed in BL21(DE3) or JM109(DE3) from a plasmid that carries *nalP* under the control of the T7 promoter (pPU300) (49). Expression of NalP was induced by the addition of IPTG (isopropyl-β-D-thiogalactopyranoside) in the growth media for 30 min to 1 h. For the detection of newly synthesized NalP on the surface of intact *N. meningitidis* cells, NalP protein was expressed in *N. meningitidis* H44/76 *nalP* from a low-copy plasmid that carries *nalP* under the control of the *lac* promoter (pEN300) (49). Plasmids pPU305 and pEN305 contain the coding sequence for a derivative of NalP that is defective in processing at the bacterial surface as a result of the mutation of Ser^{427} to Ala (49). For the detection of newly synthesized LbpA on the surface of intact *N. meningitidis* cells, LbpA protein was expressed in *N. meningitidis* CE1449, which is an *lbpA* mutant derivative of H44/76, from a plasmid that carries *lbpA* from *N. meningitidis* strain BNCV under the control of the *lac* promoter (pFP10-$lbpA_{BNCV}$). After growth of the strains in medium containing glucose, the expression of NalP or LbpA was induced by the addition of IPTG to 0.2 mM. Samples were taken before induction and at specified times after induction. Bacteria were recovered by centrifugation and fixed by resuspension with 2% formaldehyde in phosphate-buffered saline. Cells

Downloaded from https://journals.asm.org/journal/jb on 07 August 2023 by 68.181.16.190.

TABLE 3. Distribution of autotransporter proteins on the surface of intact bacteria

Autotransporter	Strain designation	Relevant genotype	Distribution of signal (% of cells)[a]	
			Polar	Circumferential
IcsA	2457T	Wild-type *S. flexneri*	98 ± 2	2 ± 2
	MBG263	*E. coli* K-12	<1	>99
SepA[b]	2457T	Wild-type *S. flexneri*	>99	<1
AIDA-I	2443 *ompT*/pIB264	*E. coli*, complete LPS	96 ± 4	4 ± 4
	MBG263/pIB264	*E. coli* K-12	1 ± 2	99 ± 2
BrkA	2443 *ompT*/pDO6935	*E. coli*, complete LPS	96 ± 5	4 ± 5
	MBG263/pDO6935	*E. coli* K-12	1 ± 2	99 ± 2
	BBC8, 1 to 2 h of induction	*B. pertussis*	67 ± 4	33 ± 4
	BBC8, >3 h of induction	*B. pertussis*	<1	>99
NalP	BL21(DE3)/pPU300	*E. coli*, complete LPS, wild-type NalP	87 ± 3	13 ± 3
	JM109(DE3)/pPU300	*E. coli* K-12, wild-type NalP	70 ± 2	30 ± 2
	BL21(DE3)/pPU305	*E. coli*, complete LPS, noncleavable NalP	33 ± 8	66 ± 8
	JM109(DE3)/pPU305	*E. coli* K-12, noncleavable NalP	17 ± 6	83 ± 6

[a] Thirty cells were tabulated in each of three independent experiments for each strain. Cells not expressing detectable levels of the protein were excluded; this represented <6% of cells for any experiment, except for BBC8 expressing BrkA (at 1 h) and BL21(DE3) expressing NalP, in which case 6 to 30% of cells did not express detectable protein.

[b] Data on SepA are from a single experiment since, for reasons that are unclear, SepA was not detected on the bacterial surface in all experiments. The data presented are from an experiment that is representative of experiments in which SepA was detected.

were then fixed onto coverslips. NalP was labeled with anti-NalP antiserum A1969F (49), and LbpA was labeled with anti-LbpA antiserum, followed by incubation with Alexa Fluor 488-conjugated goat anti-rabbit secondary antibody. Cellular DNA was stained with propidium iodide.

Expression of arabinose-inducible green fluorescent protein (GFP) fusions to derivatives of IcsA and SepA was performed essentially as described previously (9, 32). Fusion protein expression was induced in exponential-phase cultures by the addition of L-arabinose to 0.2%, followed by growth at 25°C for 30 min. Cells were mounted on agarose-coated microscope slides and imaged within 10 min, as described previously (9, 32). Each fusion protein used in the present study, including $SepA_{1\text{-}24/57\text{-}1042}$-GFP, was stable, as determined by Western blot analysis (data not shown). In contrast, $SepA_{57\text{-}1042}$-GFP was unstable, which explains the previously published observation that it displayed a diffuse fluorescent signal in the cell (9).

Microscopy. Fluorescence and phase microscopy of *S. flexneri*, *E. coli*, and *Bordetella* spp. was performed by using a ×100 oil immersion objective lens on a Nikon TE300 microscope with Nikon or Chroma Technology filters. Images were captured digitally using a black and white Photometrics Sensys or CoolSnap HQ charge-coupled device camera and IP Laboratory (Scanalytics) software. Signal intensity along the long axis of individual cells was measured on 12-bit digital images using IP Laboratory software. Fluorescence microscopy of *N. meningitidis* samples was performed on a Zeiss Axioskop, using a ×100 oil immersion objective lens and Zeiss filters. Images were captured with a Nikon DXM1200 digital camera and Nikon ACT1 software. Color figures were assembled by separately capturing signals with each of the appropriate filter sets and digitally pseudocoloring the images using Adobe Photoshop software. Tabulation of protein localization, which was conducted in a blinded fashion, and determination of the statistical significance of the observed differences were performed as described previously (32).

RESULTS AND DISCUSSION

Polar localization of the enterobacterial autotransporters IcsA, SepA, and AIDA-I. The autotransporter IcsA (VirG) of the intestinal pathogen *S. flexneri* mediates the assembly of a polarized actin tail that propels the pathogen through the cytoplasm of infected colonic mucosa cells (17). IcsA is secreted at the bacterial pole (7, 9), where it forms a polar cap on most cells (Fig. 1B and H and Table 3). We investigated whether the pole might serve as the site of secretion of autotransporter proteins more generally. The *S. flexneri* autotransporter SepA, a 150-kDa serine protease, is the most abundant protein secreted by *S. flexneri* (2). Probing of intact wild-type *S. flexneri* with antiserum to SepA revealed punctate foci at the bacterial pole (Fig. 1C and H). Essentially all cells that were associated with a detectable signal displayed SepA at only one end (Table 3), similar to the pattern seen for IcsA, which localizes preferentially to the older pole (18). Simultaneous labeling for IcsA and SepA revealed that the two proteins were present at the same pole (Fig. 1D).

The signal from SepA was more spatially restricted than that from IcsA, which frequently covered the entire hemispherical portion of the bacterial pole. Since many autotransporters exposed at the cell surface are proteolytically processed at the junction of the functional domain and the outer-membrane-embedded translocation domain (23), we examined whether the observed difference between the distribution of IcsA and that of SepA was due to a difference in the rate of proteolytic processing in conjunction with the known slow rate of diffusion of proteins in the outer membrane (39). SepA was virtually undetectable in whole-cell lysates of wild-type *S. flexneri*, indicating its efficient cleavage at the cell surface, whereas IcsA was present in greater amounts in whole-cell lysates than in the culture supernatant, indicating its relatively inefficient cleavage (Fig. 2). SepA detected on intact cells may represent cleaved protein that is maintained at the cell surface by fixation but washed away during whole-cell lysate preparations. Consistent with this, we were unable to detect SepA at the cell surface when intact *S. flexneri* organisms were probed with antibodies and washed prior to fixation (data not shown). When expressed in wild-type *E. coli*, the detection of SepA on the bacterial surface, its insertion into the outer membrane, and its proteolytic processing at the cell surface were similar to that in *S. flexneri* (data not shown). These results are consistent with the

Downloaded from https://journals.asm.org/journal/jb on 07 August 2023 by 68.181.16.190.

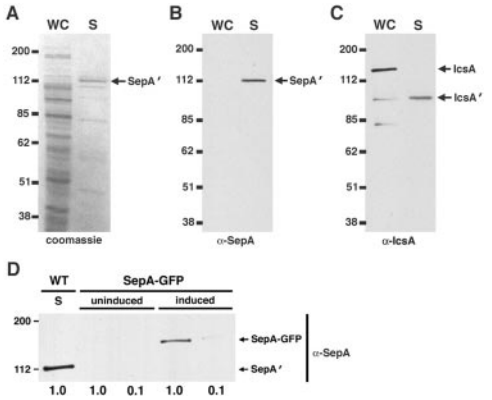

FIG. 2. Cleavage and levels of expression of *S. flexneri* SepA and IcsA. (A to C) SepA is cleaved more efficiently from the bacterial surface than IcsA. Whole-cell lysates (WC) and culture supernatant proteins (S) of *S. flexneri* wild-type strain 2457T. (A) Coomassie blue-stained gel; (B) Western blot analysis with antiserum to SepA; (C) Western blot analysis with antiserum to IcsA. The protein loaded into each lane was derived from the same volume of bacterial culture as used to derive that loaded into each other lane. (D) Comparison of the levels of expression of native SepA in the culture supernatant of *S. flexneri* wild-type strain 2457T (WT, S) to SepA-GFP in virulence plasmid-cured *S. flexneri* BS103 (SepA-GFP). SepA-GFP expression was either not induced (uninduced) or induced as in experiments shown in Fig. 1J (induced). Loading relative to wild-type *S. flexneri* supernatant proteins is shown below the blot. SepA′, cleaved functional domain of SepA; IcsA, full-length mature IcsA; IcsA′, cleaved functional domain of IcsA. Positions of molecular mass standard proteins are indicated in kilodaltons at the left of each panel.

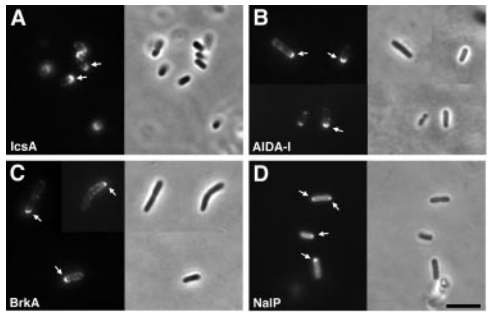

FIG. 3. Distribution of autotransporter proteins as detected by labeling bacteria live prior to fixation. (A) *S. flexneri* autotransporter IcsA on the surface of intact *S. flexneri* (strain 2457T). (B) Diffusely adherent *E. coli* autotransporter AIDA-I on the surface of intact *E. coli* 2443 cells (strain 2443 *ompT* pIB264), which express a complete LPS. (C) *Bordetella* autotransporter BrkA on the surface of intact *E. coli* 2443 cells (strain 2443 *ompT* pDO6935). (D) *N. meningitidis* autotransporter NalP on the surface of intact *E. coli* BL21(DE3) cells [strain BL21(DE3)/pPU300], which expresses a complete LPS. Arrows, polarly localized autotransporter protein. Left panel, fluorescence image; right panel, phase-contrast image. Size bar, 5 μm.

translocation to the bacterial surface of newly synthesized IcsA and SepA occurring in the same focal area of the polar outer membrane, with more rapid proteolytic release of SepA than IcsA from the cell surface.

We next demonstrated that AIDA-I, a 132-kDa autotransporter that mediates adhesion to human cells by pathogenic diffusely adherent *E. coli* (DAEC) strains (4), also localizes to the bacterial pole. AIDA-I, constitutively expressed from plasmid pIB264, localized to polar caps on the surface of wild-type *E. coli* (Fig. 1E and H). AIDA-I was polar on 96% ± 4% of cells (Table 3). As for all autotransporters examined in the present study, with the exception of SepA (see above), the detection of AIDA-I at the pole was not a result of the fixation methods used, since an identical distribution was seen when antibody labeling was performed on live cells prior to fixation (Fig. 3). Thus, autotransporters of the related *Enterobacteriaceae E. coli* and *S. flexneri* contain information that localizes them to the poles of these organisms.

The localization of AIDA-I we observed differs from that of a previous report in which AIDA-I expressed from a plasmid in a K-12 strain of *E. coli* was found distributed evenly over the bacterial surface (5). In a separate study, another *E. coli* autotransporter, antigen 43, was also distributed evenly over the surface of *E. coli* K-12 (20). A potentially significant difference between those studies and the findings reported here is that, in those studies, the autotransporters were expressed in K-12 strains of *E. coli*, which synthesize an incomplete lipopolysaccharide (LPS), whereas here, we expressed AIDA-I in a strain of *E. coli* that has complete LPS (41). For at least a subgroup of proteins with large extracellular domains, the rates of diffusion in the outer membrane of bacteria that express incomplete LPS are increased (37, 39). Hence, after its secretion at the pole, IcsA expressed in *E. coli* K-12 diffuses in the outer membrane, distributing it around the cell on >99% of cells (Fig. 1F and H and Table 3) (7, 19). IcsA expressed from the same plasmid and under the same conditions is polar on the surface of an *E. coli* strain that has a complete LPS (data not shown) (32). To determine whether the composition of the LPS might explain the difference between our observations and those previously published, we examined the distribution of AIDA-I expressed in *E. coli* K-12 strain MBG263 in a manner identical to how it was expressed in wild-type *E. coli* strain 2443 that has a complete LPS. In *E. coli* K-12, AIDA-I was distributed diffusely around 99% ± 2% of cells (Fig. 1G and H and Table 3), indicating that the uniform distribution of AIDA-I described in the earlier report likely resulted from diffusion of polarly secreted protein in the outer membrane.

Polar localization of the *Bordetella* autotransporter BrkA. We examined the localization of the 103-kDa autotransporter BrkA of the more distantly related gram-negative coccobacillary pathogen *Bordetella*. It has been shown previously that, as occurs in *Bordetella*, in *E. coli* BrkA inserts into the outer membrane and is proteolytically processed at the bacterial surface, whereupon the cleaved extracellular domain remains tightly associated with the translocator domain (33). When constitutively expressed from plasmid pDO6935 in wild-type *E. coli*, BrkA was detected in polar caps on the surface of 96% ± 5% of intact organisms (Fig. 4A and G and Table 3), indicating that BrkA contains the information required for its localization to the pole of *E. coli*. As for AIDA-I, maintenance of this distribution was dependent on an intact LPS, since when expressed from the same plasmid in *E. coli* K-12, BrkA was present around the periphery of 99% ± 2% of cells (Fig. 4B and Table 3). This result is consistent with a prior report in which BrkA expressed from the same plasmid in another *E. coli* K-12 strain was also distributed diffusely on the cell surface (33).

To test whether *Bordetella* species carry the positional infor-

Downloaded from https://journals.asm.org/journal/jb on 07 August 2023 by 68.181.16.190.

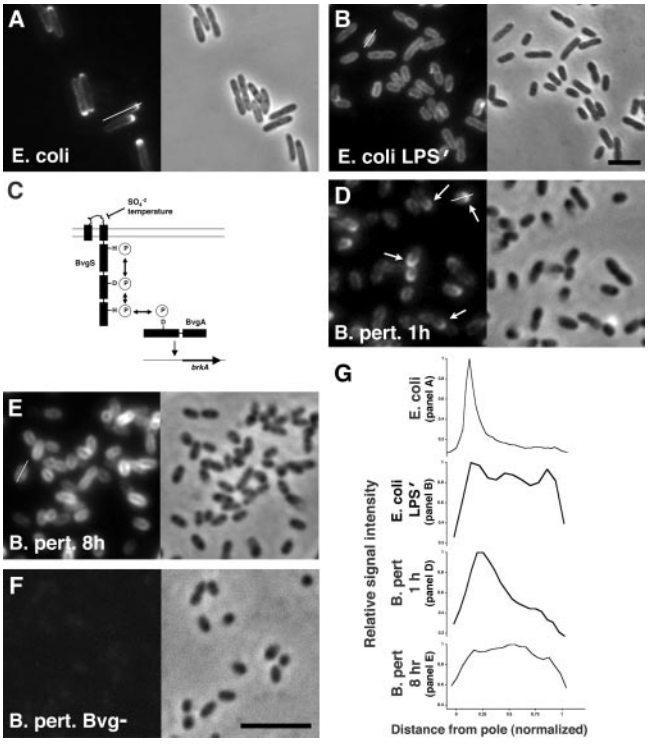

FIG. 4. Localization of the *Bordetella* autotransporter BrkA to the bacterial pole. (A and B) BrkA on the surface of intact *E. coli* cells (strain 2443 *ompT*/pDO6935), which express a complete LPS (A), or on the surface of intact *E. coli* K-12 (strain MBG263/pDO6935) (B). (C) Schematic of the *Bordetella* BvgAS two-component signal transduction pathway, which controls *brkA* transcription in response to environmental stimuli. (D) Newly synthesized BrkA on the surface of intact *B. pertussis* (strain BBC8). Cells were harvested after 1 h of growth in Bvg^+ conditions. (E) BrkA on the surface of intact *B. pertussis* (strain BBC8) after 8 h of growth in Bvg^+ conditions. (F) Absence of BrkA on the surface of *B. pertussis* (strain BBC8) following growth under Bvg^- conditions. (G) Plots of signal intensity (*y* axis) as a function of distance from cell pole along the long axis (*x* axis) for representative single cells (indicated by a white line) from each of panels A and B and D to E. B. pert, *B. pertussis*; arrows, protein detected at one pole. A and B and D to F: left panel, fluorescence image; right panel, phase-contrast image. Size bars, 5 μm.

mation that is required for localization of BrkA to the pole, we examined its localization in wild-type *B. pertussis*. Since the LPS of *B. pertussis* is truncated (often referred to as lipooligosaccharide) (44), to minimize the effect of diffusion of the molecule in the outer membrane, we examined the distribution of newly synthesized native BrkA. We took advantage of the inherent Bvg two-component signal transduction system, which controls the transcription of a set of *Bordetella* genes, including *brkA*, in response to environmental cues. At 30°C and in the presence of sulfate ions, transcription of *brkA* is repressed, whereas at 37°C and in the absence of sulfate, *brkA* transcription is activated by the response regulator BvgA (Fig. 4C) (44). After 1 to 2 h of growth under inducing conditions, newly synthesized BrkA was detected on the *B. pertussis* surface in a polar cap on 67% ± 4% of cells and diffusely around the periphery of 33% ± 4% of cells (Fig. 4D and G and Table 3). After more than 3 h of induction of BrkA expression, the signal was detected diffusely around the periphery of >99% of *B. pertussis* cells (Fig. 4E and G and Table 3). In the absence of induction, only low-level signal consistent with nonspecific binding of antibody to the bacteria was detected (Fig. 4F). As for *S. flexneri* IcsA and *E. coli* AIDA-I, these patterns of localization are consistent with the secretion of BrkA across the outer membrane occurring at the pole but with lack of its maintenance at the pole in the presence of short LPS oligosaccharide. Thus, *B. pertussis*, like *S. flexneri* and *E. coli*, carries the positional information that is required for the localization of autotransporters to the pole.

Localization of NalP, an autotransporter from spherically shaped *N. meningitidis*, at the pole of *E. coli*. In contrast to bacillary and coccobacillary bacteria, coccal bacteria, which are nearly spherical, lack clearly defined poles. To test whether autotransporters of gram-negative cocci might nevertheless contain information required for asymmetric secretion, we examined the localization of the 119-kDa *N. meningitidis* autotransporter NalP upon its expression from plasmid pPU300 in *E. coli* with a complete LPS. It has been shown previously that, when expressed from pPU300 in *E. coli*, NalP is inserted into the outer membrane such that the extracellular domain is gradually processed and released into the culture supernatant, leaving some full-length NalP associated with the cell pellet (49). Under these conditions, the signal from NalP was restricted to the poles of 87% ± 3% of bacteria (Fig. 5A and Table 3), indicating that, like the autotransporters of bacillary and coccobacillary bacteria examined here, NalP contains information required for localization to the pole of *E. coli*. The restriction of NalP to the *E. coli* pole was less dependent on the presence of a complete LPS than was restriction of other autotransporters to the pole, since in *E. coli* K-12, NalP was polar in 70% ± 2% of cells (Table 3), which may be due in part to relatively efficient proteolytic cleavage of NalP at the bacterial surface. Consistent with this, a derivative of NalP that is defective in autoproteolytic processing at the bacterial surface and therefore accumulates in the outer membrane (NalP $S^{427}A$, expressed identically to the wild-type NalP described above) gave a less polar distribution than cleaved NalP upon expression in either *E. coli* with a complete LPS or *E. coli* K-12 (Table 3). Thus, the ability to localize to the pole of *E. coli* or the pole of closely related *Shigella* is widely conserved among autotransporter proteins, including autotransporters native to coccal organisms.

Localization of NalP in distinct foci on the surface of *N. meningitidis*. To test whether in the neisserial coccus, localization of NalP is asymmetric, we examined the distribution of NalP on the surface of *N. meningitidis*. Since, like the LPS of *B. pertussis*, the LPS of *Neisseria* spp. is truncated, we visualized the sites of localization of NalP on the bacterial surface soon after its synthesis. This was accomplished by controlling *nalP* expression from an IPTG-inducible promoter on low-copy plasmid pEN300. In wild-type *N. meningitidis*, due to its efficient proteolytic cleavage at the bacterial surface, full-length NalP is barely detectable in whole-cell protein preparations (Fig. 6C). Expression of *nalP* from pEN300 increased the level of expression severalfold above native levels and thereby led to the accumulation of some full-length NalP in whole-cell protein preparations (Fig. 6C), which could also be detected on the bacterial surface (Fig. 5B). At early times after the induction of its expression, NalP was detected on the bacterial sur-

Downloaded from https://journals.asm.org/journal/jb on 07 August 2023 by 68.181.16.190.

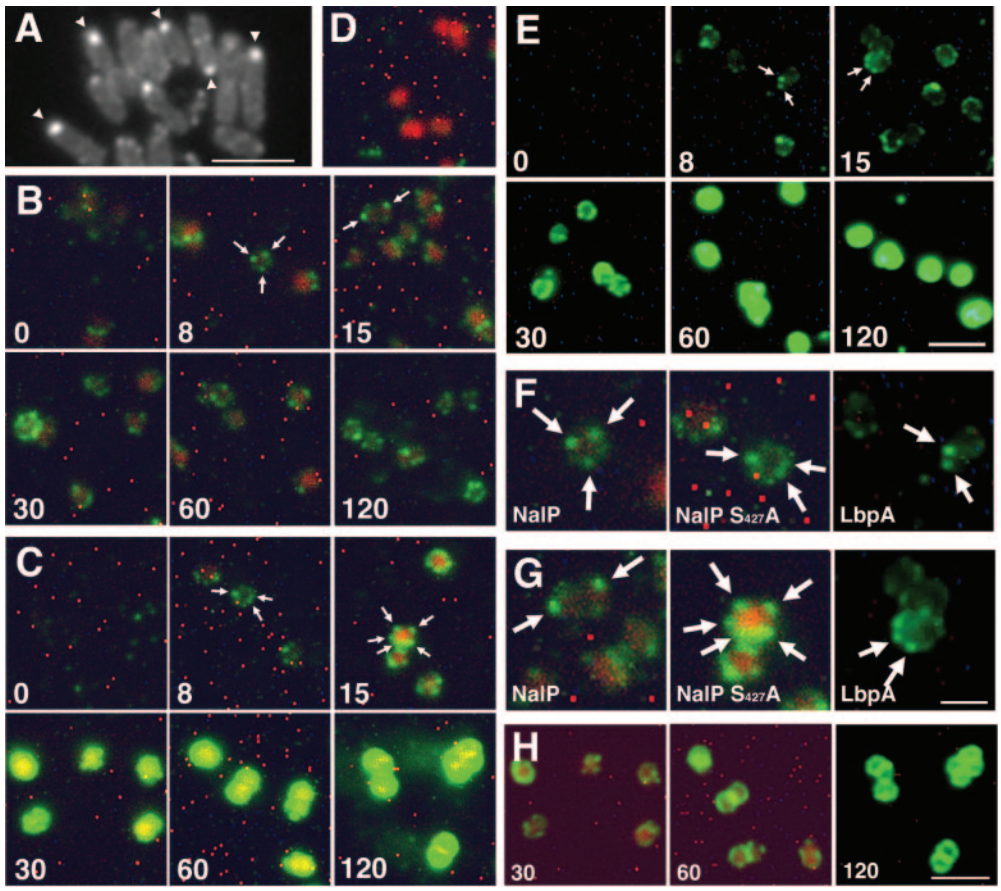

FIG. 5. Localization of the *N. meningitidis* autotransporter NalP and integral outer membrane protein LbpA. (A) NalP on the surface of intact *E. coli* cells [strain BL21(DE3)/pPU300]. Arrowheads, NalP at the bacterial pole. (B) Newly synthesized NalP on the surface of *N. meningitidis* (strain H44/76 *nalP*/pEN300). (C) Newly synthesized NalP $S^{427}A$ derivative, which is not proteolytically processed, at the surface of *N. meningitidis* (strain H44/76 *nalP* pEN305). (D) Absence of detectable NalP on the surface of an *N. meningitidis nalP* mutant (strain H44/76 *nalP*). (E) Newly synthesized LbpA on the surface of *N. meningitidis* (strain CE1449/pFP10-$lbpA_{BNCV}$). (F) Enlargement of 8-min time points of panels B to E. (G) Enlargement of 15-min time points of panels B to E. (H) Lower signal level of late time points of panel C. (B to E) Green, NalP (B to D) or LbpA (E), by indirect immunofluorescence. (B to D) Red, propidium iodide staining of bacterial DNA. Numbers indicate the time (in minutes) of induction of *nalP* (B to D) or *lbpA* (E) expression from a *lac* promoter by the addition of IPTG. Arrows indicate the foci of NalP (B and C) or LbpA (E) on the bacterial surface. Size bars: A, 5 μm; B to E (bar shown in panel E), 5 μm; F and G (bar shown in panel G), 2 μm; H, 5 μm.

face in distinct foci (Fig. 5B, F, and G). Each cell displayed one or more foci that were scattered over the cell surface; no particular pattern of distribution was discernible. As expected, in a strain that expressed a derivative of NalP that is defective in autoproteolytic processing at the bacterial surface (NalP $S^{427}A$; Fig. 6), the fluorescent signal increased with length of induction (Fig. 5C versus 5B) and became more diffuse, even when the signal intensity was reduced (Fig. 5H), which is consistent with an accumulation of NalP in the outer membrane. It was not possible to determine whether an observed increase in the number of foci on cells expressing NalP $S^{427}A$ resulted from newly synthesized NalP being secreted at new sites or from lateral diffusion in the outer membrane of NalP $S^{427}A$ that had been secreted at an earlier time. In a *nalP* mutant strain or in the absence of induction, no NalP was detected either associated with cells or by Western blot analysis (Fig. 5 and 6). These data are consistent with the secretion of NalP occurring at distinct foci rather than uniformly throughout the cell envelope.

In distinction to the polar localization of autotransporters in rod-shaped cells, NalP appears to localize to multiple sites that are not strictly analogous to cell poles. However, in *Neisseria* spp., because the cell division septum forms perpendicular to the planes in which it formed during each of the prior two cell division events (52), the portion of the cell envelope that would be analogous to the pole of a rod-shaped cell differs with successive cell division events. Therefore, the localization of neisserial autotransporters at multiple distinct sites around the coccus might reflect the complex history of the cell envelope and its relationship to the cell division site.

To address whether the foci in which NalP is localized might represent specific sites of secretion of autotransporters in *N. meningitidis*, we determined the distribution of an outer membrane protein that is not an autotransporter, the lactoferrin receptor integral outer membrane component LbpA. We examined the localization of newly synthesized LbpA on the bacterial surface by using the methods used for NalP; under these conditions, the amount of LbpA in the cell, as determined by Western blotting of whole-cell lysates, was comparable to those of native LbpA associated with *N. meningitidis*

Downloaded from https://journals.asm.org/journal/jb on 07 August 2023 by 68.181.16.190.

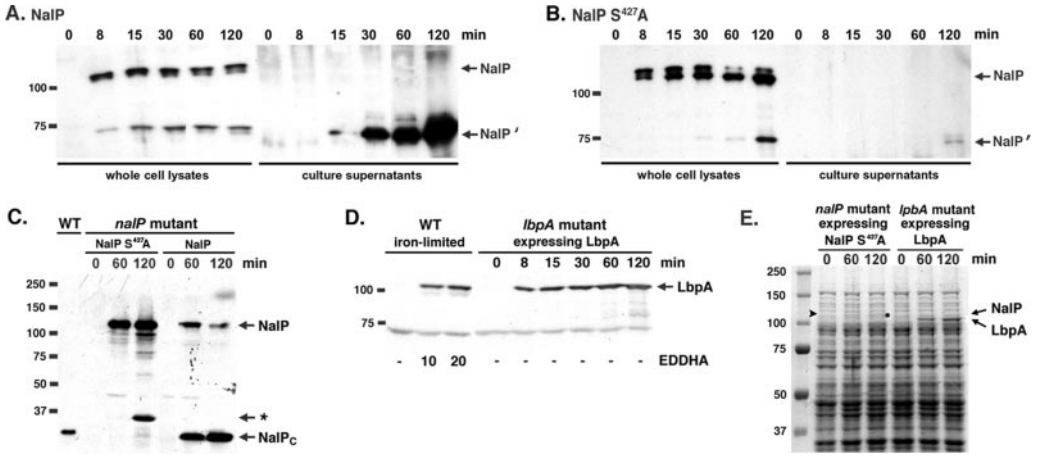

FIG. 6. Levels of expression of *N. meningitidis* proteins. (A to C) Newly synthesized NalP at early times after induction of *nalP* expression in *N. meningitidis*, as detected by Western blot analysis. (A) Wild-type NalP expressed from the *lac* promoter (strain H44/76 *nalP*/pEN300); antibody to the NalP functional domain; (B) NalP $S^{427}A$, which is nonautocleavable, expressed from the *lac* promoter (strain H44/76 *nalP* pEN305); antibody to the NalP functional domain. (C) Amounts of NalP $S^{427}A$ and cleavable NalP upon their overexpression in *nalP* mutant *N. meningitidis* relative to the amount of NalP in wild-type *N. meningitidis* (WT), all of which is cleaved; antibody to NalP carboxy-terminal translocation domain. (D) Amount of LbpA upon its expression in *lbpA* mutant of *N. meningitidis* relative to the amount of LbpA in wild-type *N. meningitidis* (WT) upon growth in iron-limiting conditions; antibody to LbpA. (E) Amount of NalP $S^{427}A$ upon its overexpression in *nalP* mutant *N. meningitidis* relative to the amount of LbpA upon its expression in *lbpA* mutant *N. meningitidis*. Coomassie blue-stained SDS-PAGE gel. Numbers above the blots and gel indicate time (in minutes) after addition the of IPTG. NalP, full-length mature NalP; NalP′, cleaved functional domain of NalP; asterisk in panel C, NalP breakdown product (49); $NalP_C$, NalP carboxy-terminal translocation domain; LbpA, full-length LbpA; EDDHA, iron chelator, with concentration (in μg/ml) given beneath the figure; arrowhead in panel E, NalP. The positions of the molecular mass standard proteins are indicated in kilodaltons at the left of each panel.

grown under iron-limiting conditions (Fig. 6D). These levels of LbpA are significantly greater than those of the noncleavable NalP expressed from pEN305, as determined by intensity of the band on a Coomassie blue-stained SDS-PAGE gel (Fig. 6E). At early times after induction, newly synthesized LbpA was detected in distinct foci that resembled those observed for both cleaved and uncleaved NalP (Fig. 5B, C, E, F, and G), consistent with the secretion of each occurring at distinct sites, rather than uniformly throughout the cell envelope. Of note, in the gram-positive coccus *Streptococcus pyogenes*, the general secretory apparatus is asymmetrically localized, albeit to a single focus per cell (40). At late times, the distribution of LbpA, which is not cleaved, was similar to that of noncleavable NalP (Fig. 5E versus 5C), which is consistent with the accumulation of each in the outer membrane. Since native full-length NalP is undetectable on *N. meningitidis* cells (Fig. 6C), in the experiments described above, the possibility that overexpression of wild-type NalP from the inducible expression vector led to its secretion at aberrant sites could not be eliminated. Nevertheless, the localization of NalP in distinct sites under these experimental conditions is not exclusive to autotransporters but is shared by at least one other large neisserial protein.

Localization of autotransporters to the bacterial pole occurs in the cytoplasm and is independent of secretion. Localization of IcsA to the pole occurs in the bacterial cytoplasm prior to secretion and independent of components of the secretion apparatus (7, 9). Consistent with this, a fusion of GFP to the functional domain of SepA localized to the cell poles of both *E. coli* strain MBG263 and an *S. flexneri* strain that has been cured of the virulence plasmid (strain BS103), on which *sepA* and *icsA* are encoded (data not shown). Furthermore, localization of GFP fusions to SepA and IcsA to the pole was independent of a functional secretion signal, since derivatives in which the Sec recognition motif within the signal peptide has been deleted formed distinct fluorescent foci at the pole in 86% ± 2% of cells expressing SepA-GFP and 89% ± 4% of cells expressing IcsA-GFP (Fig. 1I and J). In this experiment, the level of expression of the SepA-GFP fusion protein, as determined with an antibody against the region of SepA that is common to SepA-GFP and native SepA, was severalfold less than the level of expression of native SepA in wild-type *S. flexneri* (Fig. 2). Therefore, its polar localization was not a result of overexpression. As we have observed previously for native IcsA on the surface of wild-type *S. flexneri* and for IcsA-GFP fusions in the cytoplasm (9), in exponential-phase cells, SepA-GFP was detected at only one pole in approximately half and at both poles in approximately half (data not shown). To test whether the localization of the SepA-GFP fusion to the pole was specific and not the result of inclusion body formation, we examined whether the simultaneous expression of untagged full-length SepA in parallel would interfere with the polar localization of the SepA-GFP. In this series of experiments (performed in strain MBG263), when SepA-GFP was expressed alone GFP foci were present at the pole in 94% ± 9% of cells, but when expressed in parallel with untagged full-length SepA the GFP foci were present at the pole in only 7% ± 1% of cells, suggesting that the localization of the SepA-GFP fusion to the pole is specific and dependent on a limiting factor. We have previously shown that untagged full-length IcsA similarly interferes with the polar localization of IcsA-GFP (9). Thus, the *S. flexneri* autotransporters IcsA and SepA are localized to the cell pole prior to secretion, indicating that the secretion of each occurs at the pole. Using similar assays, we were unable to demonstrate that full-length SepA interferes with localization

Downloaded from https://journals.asm.org/journal/jb on 07 August 2023 by 68.181.16.190.

of IcsA-GFP or that full-length IcsA interferes with localization of SepA-GFP (data not shown); thus, we were unable to definitively determine whether the two proteins recognize a common factor.

Our data demonstrate that a wide variety of autotransporters localize to the pole of rod-shaped bacteria. The restriction of autotransporters to the pole is dependent on the presence of a complete LPS. Newly synthesized and secreted BrkA is polar even in the presence of truncated LPS, and secretion-incompetent fusions of GFP to IcsA and SepA are polar in the bacterial cytoplasm. Together, these findings strongly suggest that the secretion of autotransporters of rod-shaped bacteria occurs at the pole. However, we cannot absolutely eliminate the possibility that polar localization of autotransporters could occur by alternate mechanisms following secretion at sites away from the pole.

In *E. coli* that expresses a complete LPS, LPS molecules are organized in a helical arrangement on the cell surface and do not diffuse freely out of the helix (15). Moreover, a subset of outer membrane proteins is stably maintained at the cell poles (11, 13, 16). It seems likely that autotransporters are among the subpopulation of outer membrane proteins that are stable at the poles. Since LPS molecules do not diffuse, a potential mechanism of maintaining autotransporters at the pole would involve interactions with LPS. Whether autotransporters interact with LPS has not been determined, and other mechanisms of maintaining autotransporters at the pole are also possible.

Given the wide evolutionary distribution of autotransporter proteins among gram-negative bacteria, our results suggest that mechanisms for localization and secretion of autotransporters at the bacterial pole are also widely present and perhaps widely conserved. Since many autotransporters are abundant among gram-negative pathogens and have important roles in the virulence of these organisms, their localization at the pole suggests that orientation of the bacterial body may at times be relevant to pathogen-host interactions for organisms that express a complete LPS.

Two other secretion systems, the type II secretion system of *Vibrio cholerae*, which translocates substrate proteins across the bacterial outer membrane, and the type IV secretion systems of *Legionella pneumophila* and *Agrobacterium tumefaciens*, which translocate substrate proteins across both bacterial membranes and a eukaryotic membrane, are localized to the bacterial pole (10, 24, 26, 42). Secretion systems homologous to these are present in a large number of gram-negative organisms, and yet the extent to which the polar localization of these systems is conserved is unknown. In contrast, the Sec secretion apparatus, which translocates substrate proteins across the bacterial inner membrane, is distributed around the cell periphery without obvious polar bias (7, 8). Whether or not the Tat secretion system, which secretes folded proteins across the bacterial inner membrane, is polar remains controversial (6, 38). Finally, the type III secretion system of gram-negative bacteria, which translocates substrate proteins across both bacterial membranes and a eukaryotic membrane, appears by electron microscopy to be present around the cell periphery without obvious polar bias (25).

In rod-shaped bacteria, whereas the Sec translocation channel is distributed uniformly in the inner membrane (7, 8), the peptidoglycan and the outer membrane are relatively inert at the pole compared to along the lengths of the cell (11, 12). The inert composition of these polar structures may be relevant to the polar secretion of autotransporters. If specific proteins or structures are required for the folding of these unusually large proteins in the periplasm and/or for their translocation across the outer membrane, the inert composition of the pole may provide a relatively stable scaffold for the assembly and maintenance of these factors. Whether similarly inert areas of the cell envelope exist in gram-negative cocci is unknown, but our observation that neisserial NalP is secreted at the pole of *E. coli* and at distinct sites in *N. meningitidis* suggests that the sites of autotransporter secretion in *N. meningitidis*, and perhaps all gram-negative cocci, may contain characteristics of the poles of gram-negative rods. Further investigation will provide insight into the mechanisms by which members of this large group of virulence proteins traverse the cell envelope. In addition, it will provide insight into the similarities and differences in the organization of the envelopes of gram-negative cocci and gram-negative rods.

ACKNOWLEDGMENTS

We thank J. Kortekaas for providing the *lbpA* expression plasmid and LbpA antiserum.

This study was supported by NIH grants AI35817 (to M.B.G.) and AI061073 (to M.B.G.), by AHA award 0325770T (to S.J.), by grants from the Deutsche Forschungsgemeinschaft DFG SFB293 TPB5 and SCHM 770/10-4 (to M.A.S.), and by Natural Sciences and Engineering Research Council of Canada grant 194599 (to R.F.).

ADDENDUM IN PROOF

Since the acceptance of the manuscript, (Shiomi et al. D. Shiomi, M. Yoshimoto, M. Homma, and I. Kawagishi, Mol. Microbiol. **60:**894–906, 2006) have presented data indicating that the Sec translocon is organized in an inner membrane helix along the length of *E. coli*.

REFERENCES

1. **Bartolome, B., Y. Jubete, E. Martinez, and F. de la Cruz.** 1991. Construction and properties of a family of pACYC184-derived cloning vectors compatible with pBR322 and its derivatives. Gene **102:**75–78.
2. **Benjelloun-Touimi, Z., P. J. Sansonetti, and C. Parsot.** 1995. SepA, the major extracellular protein of *Shigella flexneri*: autonomous secretion and involvement in tissue invasion. Mol. Microbiol. **17:**123–135.
3. **Benz, I., and M. A. Schmidt.** 1992. AIDA-I, the adhesin involved in diffuse adherence of the diarrhoeagenic *Escherichia coli* strain 2787 (O126:H27), is synthesized via a precursor molecule. Mol. Microbiol. **6:**1539–1546.
4. **Benz, I., and M. A. Schmidt.** 1989. Cloning and expression of an adhesin (AIDA-I) involved in diffuse adherence of enteropathogenic *Escherichia coli*. Infect. Immun. **57:**1506–1511.
5. **Benz, I., and M. A. Schmidt.** 1992. Isolation and serologic characterization of AIDA-I, the adhesin mediating the diffuse adherence phenotype of the diarrhea-associated *Escherichia coli* strain 2787 (O126:H27). Infect. Immun. **60:**13–18.
6. **Berthelmann, F., and T. Bruser.** 2004. Localization of the Tat translocon components in *Escherichia coli*. FEBS Lett. **569:**82–88.
7. **Brandon, L. D., N. Goehring, A. Janakiraman, A. W. Yan, T. Wu, J. Beckwith, and M. B. Goldberg.** 2003. IcsA, a polarly-localized autotransporter with an atypical signal peptide, uses the Sec apparatus for secretion, although the Sec apparatus is circumferentially distributed. Mol. Microbiol. **50:**45–60.
8. **Campo, N., H. Tjalsma, G. Buist, D. Stepniak, M. Meijer, M. Veenhuis, M. Westermann, J. P. Muller, S. Bron, J. Kok, O. P. Kuipers, and J. D. Jongbloed.** 2004. Subcellular sites for bacterial protein export. Mol. Microbiol. **53:**1583–1599.
9. **Charles, M., M. Perez, J. H. Kobil, and M. B. Goldberg.** 2001. Polar targeting of *Shigella* virulence factor IcsA in *Enterobacteriaceae* and *Vibrio*. Proc. Natl. Acad. Sci. USA **98:**9871–9876.
10. **Conover, G. M., I. Derre, J. P. Vogel, and R. R. Isberg.** 2003. The *Legionella pneumophila* LidA protein: a translocated substrate of the Dot/Icm system

Downloaded from https://journals.asm.org/journal/jb on 07 August 2023 by 68.181.16.190.

associated with maintenance of bacterial integrity. Mol. Microbiol. **48:**305–321.
11. **de Pedro, M. A., C. G. Grunfelder, and H. Schwarz.** 2004. Restricted mobility of cell surface proteins in the polar regions of *Escherichia coli*. J. Bacteriol. **186:**2594–2602.
12. **de Pedro, M. A., J. C. Quintela, J. V. Holtje, and H. Schwarz.** 1997. Murein segregation in *Escherichia coli*. J. Bacteriol. **179:**2823–2834.
13. **de Pedro, M. A., K. D. Young, J. V. Holtje, and H. Schwarz.** 2003. Branching of *Escherichia coli* cells arises from multiple sites of inert peptidoglycan. J. Bacteriol. **185:**1147–1152.
14. **Fernandez, R. C., and A. A. Weiss.** 1994. Cloning and sequencing of a *Bordetella pertussis* serum resistance locus. Infect. Immun. **62:**4727–4738.
15. **Ghosh, A. S., and K. D. Young.** 2005. Helical disposition of proteins and lipopolysaccharide in the outer membrane of *Escherichia coli*. J. Bacteriol. **187:**1913–1922.
16. **Gibbs, K. A., D. D. Isaac, J. Xu, R. W. Hendrix, T. J. Silhavy, and J. A. Theriot.** 2004. Complex spatial distribution and dynamics of an abundant *Escherichia coli* outer membrane protein, LamB. Mol. Microbiol. **53:**1771–1783.
17. **Goldberg, M. B.** 2001. Actin-based motility of intracellular microbial pathogens. Microbiol. Mol. Biol. Rev. **65:**595–626.
18. **Goldberg, M. B., O. Barzu, C. Parsot, and P. J. Sansonetti.** 1993. Unipolar localization and ATPase activity of IcsA, a *Shigella flexneri* protein involved in intracellular movement. J. Bacteriol. **175:**2189–2196.
19. **Goldberg, M. B., and J. A. Theriot.** 1995. *Shigella flexneri* surface protein IcsA is sufficient to direct actin-based motility. Proc. Natl. Acad. Sci. USA **92:**6572–6576.
20. **Henderson, I. R., M. Meehan, and P. Owen.** 1997. Antigen 43, a phase-variable bipartite outer membrane protein, determines colony morphology and autoaggregation in *Escherichia coli* K-12. FEMS Microbiol. Lett. **149:**115–120.
21. **Henderson, I. R., and J. P. Nataro.** 2001. Virulence functions of autotransporter proteins. Infect. Immun. **69:**1231–1243.
22. **Henderson, I. R., F. Navarro-Garcia, M. Desvaux, R. C. Fernandez, and D. Ala'Aldeen.** 2004. Type V protein secretion pathway: the autotransporter story. Microbiol. Mol. Biol. Rev. **68:**692–744.
23. **Henderson, I. R., F. Navarro-Garcia, and J. P. Nataro.** 1998. The great escape: structure and function of the autotransporter proteins. Trends Microbiol. **6:**370–378.
24. **Judd, P. K., R. B. Kumar, and A. Das.** 2005. Spatial location and requirements for the assembly of the *Agrobacterium tumefaciens* type IV secretion apparatus. Proc. Natl. Acad. Sci. USA **102:**11498–11503.
25. **Kubori, T., A. Sukhan, S. I. Aizawa, and J. E. Galan.** 2000. Molecular characterization and assembly of the needle complex of the *Salmonella typhimurium* type III protein secretion system. Proc. Natl. Acad. Sci. USA **97:**10225–10230.
26. **Kumar, R. B., and A. Das.** 2002. Polar location and functional domains of the *Agrobacterium tumefaciens* DNA transfer protein VirD4. Mol. Microbiol. **43:**1523–1532.
27. **LaBrec, E. H., H. Schneider, T. J. Magnani, and S. B. Formal.** 1964. Epithelial cell penetration as an essential step in the pathogenesis of bacillary dysentery. J. Bacteriol. **88:**1503–1518.
28. **Magdalena, J., and M. B. Goldberg.** 2002. Quantification of *Shigella* IcsA required for bacterial actin polymerization. Cell Motil. Cytoskeleton **51:**187–196.
29. **Maurelli, A. T., B. Blackmon, and R. Curtiss III.** 1984. Loss of pigmentation in *Shigella flexneri* 2a is correlated with loss of virulence and virulence-associated plasmid. Infect. Immun. **43:**397–401.
30. **Meissner, P. S., W. P. Sisk, and M. L. Berman.** 1987. Bacteriophage lambda cloning system for the construction of directional cDNA libraries. Proc. Natl. Acad. Sci. USA **84:**4171–4175.
31. **Morona, R., and L. Van Den Bosch.** 2003. Lipopolysaccharide O antigen chains mask IcsA (VirG) in *Shigella flexneri*. FEMS Microbiol. Lett. **221:**173–180.
32. **Nilsen, T., A. S. Ghosh, M. B. Goldberg, and K. D. Young.** 2004. Branching sites and morphological abnormalities behave as ectopic poles in shape-defective *Escherichia coli*. Mol. Microbiol. **52:**1045–1054.
33. **Oliver, D. C., G. Huang, and R. C. Fernandez.** 2003. Identification of secretion determinants of the *Bordetella pertussis* BrkA autotransporter. J. Bacteriol. **185:**489–495.
34. **Oomen, C. J., P. Van Ulsen, P. Van Gelder, M. Feijen, J. Tommassen, and P. Gros.** 2004. Structure of the translocator domain of a bacterial autotransporter. EMBO J. **23:**1257–1266.
35. **Pallen, M. J., R. R. Chaudhuri, and I. R. Henderson.** 2003. Genomic analysis of secretion systems. Curr. Opin. Microbiol. **6:**519–527.
36. **Pettersson, A., T. Prinz, A. Umar, J. van der Biezen, and J. Tommassen.** 1998. Molecular characterization of LbpB, the second lactoferrin-binding protein of *Neisseria meningitidis*. Mol. Microbiol. **27:**599–610.
37. **Rajakumar, K., B. H. Jost, C. Sasakawa, N. Okada, M. Yoshikawa, and B. Adler.** 1994. Nucleotide sequence of the rhamnose biosynthetic operon of *Shigella flexneri* 2a and role of lipopolysaccharide in virulence. J. Bacteriol. **176:**2362–2373.
38. **Ray, N., A. Nenninger, C. W. Mullineaux, and C. Robinson.** 2005. Location and mobility of twin arginine translocase subunits in the *Escherichia coli* plasma membrane. J. Biol. Chem. **280:**17961–17968.
39. **Robbins, J. R., D. Monack, S. J. McCallum, A. Vegas, E. Pham, M. B. Goldberg, and J. A. Theriot.** 2001. The making of a gradient: IcsA (VirG) polarity in *Shigella flexneri*. Mol. Microbiol. **41:**861–872.
40. **Rosch, J., and M. Caparon.** 2004. A microdomain for protein secretion in gram-positive bacteria. Science **304:**1513–1515.
41. **Sandlin, R. C., and A. T. Maurelli.** 1999. Establishment of unipolar localization of IcsA in *Shigella flexneri* 2a is not dependent on virulence plasmid determinants. Infect. Immun. **67:**350–356.
42. **Scott, M. E., Z. Y. Dossani, and M. Sandkvist.** 2001. Directed polar secretion of protease from single cells of *Vibrio cholerae* via the type II secretion pathway. Proc. Natl. Acad. Sci. USA **98:**13978–13983.
43. **Sijbrandi, R., M. L. Urbanus, C. M. ten Hagen-Jongman, H. D. Bernstein, B. Oudega, B. R. Otto, and J. Luirink.** 2003. Signal recognition particle (SRP)-mediated targeting and Sec-dependent translocation of an extracellular *Escherichia coli* protein. J. Biol. Chem. **278:**4654–4659.
44. **Smith, A. M., C. A. Guzman, and M. J. Walker.** 2001. The virulence factors of *Bordetella pertussis*: a matter of control. FEMS Microbiol. Rev. **25:**309–333.
45. **Stainer, D. W., and M. J. Scholte.** 1970. A simple chemically defined medium for the production of phase I *Bordetella* pertussis. J. Gen. Microbiol. **63:**211–220.
46. **Steinhauer, J., R. Agha, T. Pham, A. W. Varga, and M. B. Goldberg.** 1999. The unipolar *Shigella* surface protein IcsA is directly targeted to the old pole; IcsP cleavage of IcsA occurs over the entire bacterial surface. Mol. Microbiol. **32:**367–378.
47. **Szabady, R. L., J. H. Peterson, K. M. Skillman, and H. D. Bernstein.** 2005. An unusual signal peptide facilitates late steps in the biogenesis of a bacterial autotransporter. Proc. Natl. Acad. Sci. USA **102:**221–226.
48. **van Ulsen, P., and J. Tommassen.** 2006. Protein secretion and secreted proteins in pathogenic *Neisseriaceae*. FEMS Microbiol. Rev. **30:**292–319.
49. **van Ulsen, P., L. van Alphen, J. ten Hove, F. Fransen, P. van der Ley, and J. Tommassen.** 2003. A neisserial autotransporter NalP modulating the processing of other autotransporters. Mol. Microbiol. **50:**1017–1030.
50. **Vollmer, W., and J. V. Holtje.** 2004. The architecture of the murein (peptidoglycan) in gram-negative bacteria: vertical scaffold or horizontal layer(s)? J. Bacteriol. **186:**5978–5987.
51. **Voulhoux, R., M. P. Bos, J. Geurtsen, M. Mols, and J. Tommassen.** 2003. Role of a highly conserved bacterial protein in outer membrane protein assembly. Science **299:**262–265.
52. **Westling-Haggstrom, B., T. Elmros, S. Normark, and B. Winblad.** 1977. Growth pattern and cell division in *Neisseria gonorrhoeae*. J. Bacteriol. **129:**333–342.

Downloaded from https://journals.asm.org/journal/jb on 07 August 2023 by 68.181.16.190.